

Adsorption and Transport of Gas-Phase Naphthalene on Micron-Size Fog Droplets in Air

SURESH RAJA AND
KALLIAT T. VALSARAJ*

Gordon A. and Mary Cain Department of
Chemical Engineering, Louisiana State University,
Baton Rouge, Louisiana 70803

Aromatic hydrocarbon vapors adsorb to the air/water interface and are transported by wet deposition processes via fog, mist, and rain. A falling droplet apparatus was used to study the adsorption and uptake of naphthalene vapor on water droplets with diameters ranging from 14 to 200 μm . Uptake of naphthalene vapor greater than that predicted by bulk (air–water) phase equilibrium was noted for diameters less than 50 μm and was attributed to surface adsorption. The experimental values of the droplet–vapor partition constants were used to obtain the mass accommodation coefficient for naphthalene at the interface. The effect of temperature on the mass accommodation coefficient was measured. The effects of a synthetic surfactant and a natural organic carbon surrogate (Suwanee Fulvic acid) on the uptake of naphthalene vapors on water droplets were also examined. Small droplet diameter, decreased temperature, and the presence of dissolved surface-active material in water enhanced the uptake of naphthalene into fog droplets.

Introduction

Polycyclic aromatic hydrocarbons (PAHs) are arguably released to the environment by anthropogenic activities such as combustion of fossil fuels, biomass burning, and even organism biosynthesis. PAHs are also said to be the most abundant class of carbon-bearing compounds in the universe (1). Many types of PAHs exist in the environment, but usually those with 3–6 aromatic benzene rings, some with alkyl substituents, are most common. These are hydrophobic and tend to accumulate in organic-rich environments such as soils, sediments, biota, and aerosols. Several of the PAHs are suspected carcinogens or mutagens; hence, their behaviors in the atmosphere with respect to deposition and reactions have been the focus of much study. They are ubiquitous contaminants in the atmosphere and have been transported to high-altitude lake sediments, deep-sea sediments, arctic ice, and snow (2–5). Although in the United States atmospheric concentrations of PAHs were found to decrease in the 1960s onward, there is evidence of an increasing trend in recent times (6). Previous work showed that in the metro Baton Rouge area a variety of PAHs exist in the ambient atmosphere (7).

There is much information in the literature on the equilibrium partitioning of compounds between the bulk water and air phases (8). The partitioning to the solids in

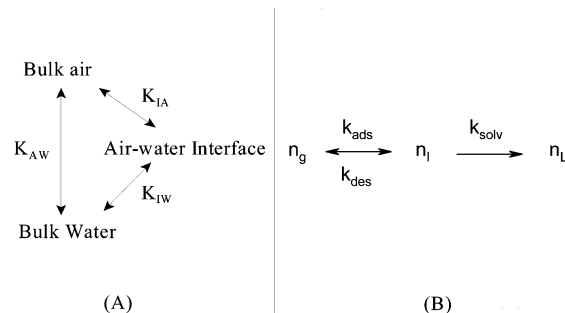


FIGURE 1. (A) Equilibrium between the bulk phases and the interface; (B) dynamics of uptake into droplets.

aerosols has also been well studied (9). A number of earlier papers have discussed the methodology of determining air–water partition constants and their importance in reaction and transport in environmental systems (10–12). Recently, data have been forthcoming on the adsorption and partitioning to the air–water interface (13–18). Water is present in the atmosphere as droplets (rain, fog, mist) and the surface area to bulk volume for these entities can be quite large. As a result the interfacial effects may become significant for the transport and reactions of PAHs. Two recent papers described the adsorption of PAHs on the air–water interface (19, 20). Previous work on the transport of PAH molecules by air bubbles in the solvent sublimation technique for wastewater treatment also showed that adsorptive transport was a significant pathway for hydrophobic molecules (20).

The equilibrium distribution of a PAH vapor between the air–water interface and the bulk phases (air, water) is handled via the Gibbs surface excess model as shown in Figure 1A, where equilibrium between air ($\equiv A$), the interface ($\equiv I$), and bulk water ($\equiv W$) are shown (22). The Gibbs surface excess identifies the equilibrium concentration at the surface as given by the changes in surface pressure with bulk air phase concentration. The surface nucleation model gives the dynamics of uptake at the interface where it is assumed that the interface is dynamic, and aggregates (i.e., a solute molecule complexed with solvent molecules) are continuously formed and dissipated (23). The surface nucleation model proposes two entities: n_i^p , the solute with a partial solvation layer, and a critical cluster, n_i^c , that is absorbed into the bulk water. The surface concentration participating in the kinetics of uptake is $n_i = n_i^p + n_i^c$. The uptake kinetics is hypothesized in Figure 1B, where the adsorption involves thermal accommodation at the surface followed by dissolution into the droplet.

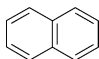
Adopting the Gibbs surface excess model, one can obtain the following standard free energy equation for equilibrium transfer between the interface and the bulk gas phase (19)

$$\Delta_A^I G^0 = -RT \ln \left(\frac{K_{IA}}{\delta_o} \right) \quad (1)$$

where K_{IA} (m) is the partition constant to the air–water interface from the bulk air given by the ratio of the surface phase to bulk air phase concentration ($= \Pi/P_a = \Gamma/C_a$), and the standard state surface thickness δ_o is 6×10^{-10} m. Estimates of K_{IA} are made either through surface pressure (A) measurements as a function of bulk gas-phase partial pressure (P_a) or using inverse gas chromatography (IGC). The surface pressure measurements are limited to compounds with large vapor pressures. PAHs are only moderately volatile and have very low vapor pressures. Hence, the inverse

* Corresponding author phone: (225)578-6522; fax: (225)578-1476; e-mail: Valsaraj@che.lsu.edu.

TABLE 1. Physicochemical Properties of Naphthalene at 298 K (19, 43)

molecular weight	128
molecular structure	
aqueous solubility	0.241 mol·m ⁻³
vapor pressure of sub-cooled liquid	0.037 kPa
air–water interfacial adsorption partition constant, K_{IA}	27.2 ± 1.8 μm
air–water bulk phase partition (Henry's law) constant, K_{WA}	53 ± 4 [-]

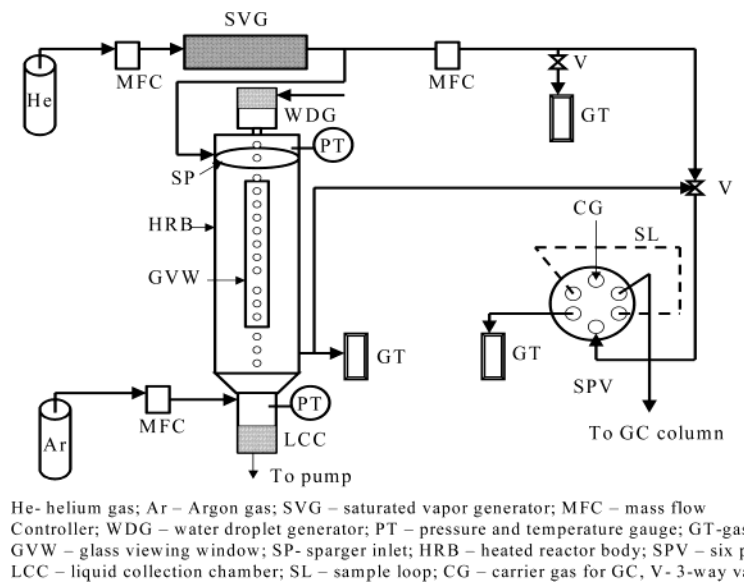


FIGURE 2. Schematic of the falling droplet apparatus used to measure the uptake and mass transfer to water droplets.

gas chromatography technique was used to obtain the thermodynamic parameters for aromatic hydrocarbons and the effects of temperature on the partitioning to the air–water interface (19). The air/water interfacial adsorption constant for naphthalene and the partition constant between the bulk phases (Henry's constant, K_{WA}) are given in Table 1. As temperature increased K_{IA} decreased, indicating that the adsorption to the air–water interface became less favorable at higher temperature. In this paper the dynamics of PAH vapor uptake into water droplets is discussed. Conventionally the uptake into droplets is calculated from the equilibrium between the bulk air and water phases. However, fogwater concentration of pesticides and organic vapors beyond that predicted by bulk phase equilibrium in the atmosphere is well documented (24, 25). The same phenomenon has also been observed in mist scrubbing technology for air pollution control (27). In an earlier work, a hypothesis was presented that adsorption to the air–water interface may explain the large concentrations of organic compounds in fog and mist droplets (26). In this work, the above hypothesis is tested. It is believed that the effects of increased partitioning to the air–water interface will become evident for those environmental systems with large surface area compared to bulk liquid volume (e.g., fog and mist which have droplet diameters of the order of 1 to 100 μm). To estimate the uptake of PAH vapors into water droplets in air we need both the equilibrium adsorption coefficient K_{IA} and the mass transfer rate coefficient, K_c for transport into the droplets. The mass transfer rate coefficient contains information on the mass accommodation coefficient, α , which gives the fraction of collisions of the gas-phase species with the surface that results in incorporation into the droplet (28–30). Although values of α have been measured for a variety of organic compounds including some aromatic compounds (33), data are nonexistent for the mass accommodation coefficients of PAH vapors. Hence, the uptake of semi-volatile

PAHs by water droplets was studied using a falling droplet apparatus that was modified from the one used for highly volatile gaseous species (32). The variation of α with temperature was also ascertained. Finally, we explored the effects of dissolved surface-active materials upon uptake that would simulate the presence of surface-active organic carbon in fog and mist.

Experimental Section

The compound considered in this work is a PAH, viz., naphthalene. The relevant physicochemical properties of the compound are given in Table 1. Naphthalene has a low vapor pressure (0.01 kPa), and is hydrophobic. Naphthalene was the volatile PAH most detected in the metro Baton Rouge atmosphere (10) and hence was chosen for this work.

Droplet uptake experiments were conducted using a falling droplet apparatus modeled after that of Jayne et al. (32) (Figure 2). A continuous, saturated stream of naphthalene vapor in helium was fed to the reactor along with a continuous stream of water droplets.

The vapor generator was made of two tubular stainless steel columns (SS 316, 0.762 m long, 0.013 m o.d.) connected serially and each packed with 15 g of Chromosorb P (60/80 mesh nonacid washed, obtained from Supelco Inc., Bellefonte, PA). The Chromosorb P was mixed with a hexane solution containing pure naphthalene (99.9%, Fisher Scientific Co., St. Louis, MO). Excess hexane was evaporated, thereby obtaining naphthalene-coated Chromosorb P. The average loading obtained this way was about 0.02 g of naphthalene per gram of support. The coated packing was supported with glass wool on both ends. To obtain reproducible carrier gas flow rates in the chamber a mass flow controller (Sierra instruments Inc., 8100 series) was used to set the helium flow rate to the saturation chamber at 55×10^{-6} m³/min.

The droplet generation assembly was made of high-density polyethylene (HDPE) with a reservoir volume of $1.16 \times 10^{-4} \text{ m}^3$. The droplets were generated using a commercially available sapphire orifice assembly (O'Keefe Controls Co., Trumbull, CT) with the desired orifice diameter (30–100 μm). A piezo-ceramic crystal (American Piezoceramics Inc., Mackeyville, PA) placed above the orifice was mechanically vibrated to generate droplets of a given size that depended on the frequency of voltage modulation (31). Distilled, deionized water was fed to the droplet generator using a model LGP pump (Graylor Dyneco Co., Cape Coral, FL). The droplets passed through a long cylindrical stainless steel reactor (0.0245 m i.d., 0.32 m long) and exited the bottom into a collection chamber. The droplet stream was photographed using a Tiffen 62-mm standard hot mirror lens connected to a desktop computer by a 30-frame-per-second interface frame grabber. The pictures were analyzed using OPTIMAS 6.2 version software. The naphthalene vapor was fed to the entrance of the reactor at the top through a porous-frit sparger placed within the reactor in the form of a perforated ring, which assured a uniform distribution of the gas stream across the cross-section of the reactor. The gas stream had naphthalene concentrations that ranged from 0.7 to 1.5 ppmv.

The uptake experiment was conducted with a constant vapor concentration of naphthalene fed to the reactor throughout the experiment, whereas the exiting liquid stream composition was determined by the residence time and mass transfer within the reactor. The liquid from the collection chamber was analyzed using liquid chromatography. The exiting gas stream at the bottom of the reactor was analyzed on-line by directing it to a gas chromatograph through a six-port sample valve. The entire reactor and the flow lines were heat traced using heating coils to maintain a constant temperature within the reactor using temperature controllers (Series 6100 from Omega Engineering Inc., Stamford, CT) and Omega model DT462 temperature indicators. The reactor pressure was maintained at ≤ 10 Torr. The reactor had two vertical glass side ports that could be used to photograph the bubbles and determine their sizes, when desired.

A Hewlett-Packard 5890 GC with a flame ionization detector was used to analyze the gas stream. A stainless steel column (0.023 m long \times 0.0063 m i.d.) packed with Chromosorb P was used for chromatographic separation. The carrier gas flow rate was 70 mL/min and column head pressure was 200 kPa (29 psi). Vapor-phase samples were injected into the GC by a manually actuated 6-port injection valve (Valco Instrument Co., Inc., Houston, TX). The injection volume for all vapor phase samples was 1 mL through a sample loop. The column temperature was 250 $^{\circ}\text{C}$. The liquid samples were analyzed using a Hewlett-Packard (Series 1100) liquid chromatograph with a diode array detector, with an Envirosep-PP HPLC column (1.25 cm long \times 0.0046 m i.d., Phenomenex, Torrance, CA).

Results and Discussion

Mass Transfer of PAH Vapor to Water Droplets in Air. For a given droplet diameter the ratio of the molar concentration of naphthalene in the water droplet [C_d] leaving the reactor to the molar concentration in the vapor phase [C_v] exiting the reactor at the bottom was obtained. This ratio is called the droplet–vapor partition constant, K_{DV} . The rate of mass transfer to the droplet is controlled by the concentration driving force between the gas stream and the droplet (35).

$$\frac{dC_d}{dt} = K_c \frac{6}{d} \left[C_v - \frac{C_d}{\left(K_{WA} + \frac{6}{d} K_{IA} \right)} \right] \quad (2)$$

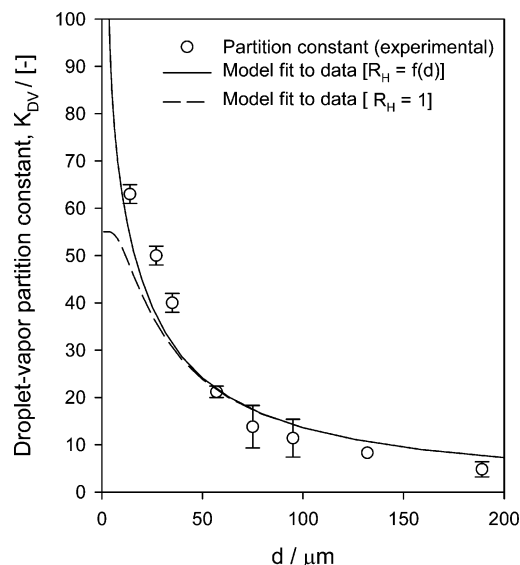


FIGURE 3. (A) Droplet–vapor partition constants (measured and fitted) versus droplet sizes for naphthalene uptake. Gas/droplet contact time = 52 ms.

Integrating the above equation with constant C_v we obtain the following equation:

$$K_{DV} = \frac{C_d}{C_v} = R_H K_{WA} \left[1 - \exp\left(-K_c \frac{1}{R_H K_{WA}} \frac{6}{d} \tau\right) \right] \quad (3)$$

where $R_H = 1 + (6/d)(K_{IA}/K_{WA})$ represents the deviation from conventional Henry's law partitioning between the bulk air and water phases. Note that K_{WA} (dimensionless molar concentration ratio) represents the vapor partitioning to the bulk water phase, whereas $(6/d)K_{IA}$ represents the vapor partitioning to the air–water interface. K_c (m/s) is the mass transfer coefficient from the vapor phase to the droplet. Note that d (m) is the droplet diameter. J (s) represents the gas/liquid contact time in the reactor and is given by u/L , where L (m) is the gas/liquid contact length in the reactor and u (m/s) is the droplet stream velocity in the reactor. The overall mass transfer coefficient, K_c (m/s) for the organic compound from vapor to the droplet in the reactor is given by the following equation (28):

$$\frac{1}{K_c} = \left(\frac{d}{2} \frac{1}{D_G} \right) + \left(\frac{4}{C} \frac{1}{\alpha} \right) + \left(\frac{1}{R_H K_{WA}} \sqrt{\frac{\pi \tau}{4 D_L}} \right) \quad (4)$$

where the three resistances, viz., gas-phase diffusion, mass accommodation at the surface, and liquid phase solubility, respectively, are represented by the three terms on the right-hand side. Note that because of limited mixing within the droplet in the reactor setting one has to consider all three resistances to be important under the laboratory experimental conditions. In the atmospheric chemistry literature K_c is also given in terms of an overall uptake coefficient, γ , so that

$$K_c = \gamma \frac{\bar{C}}{4}$$

In the above equation, \bar{C} is the average thermal speed of the molecule in the gas phase (222 m/s for naphthalene) and α is the mass accommodation coefficient that determines the probability that a molecule striking the surface will be transferred to the droplet (28). D_G ($= 5.7 \times 10^{-4} \text{ m}^2/\text{s}$) and D_L ($= 7 \times 10^{-10} \text{ m}^2/\text{s}$) are, respectively, the gas-phase and the liquid-phase diffusion constants of naphthalene. Note that as per eq 3, the ratio K_{DV} is a function of the droplet diameter, d , through R_H and the gas/liquid contact time. The droplet

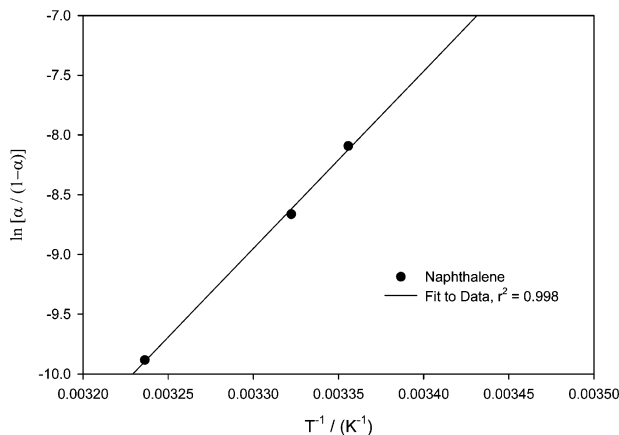


FIGURE 4. Plot of $\ln[\alpha/(1-\alpha)]$ versus $1/T$ naphthalene.

diameters in the single droplet apparatus were obtained experimentally as described earlier and were in agreement with the relationship $d = 1.89d_{\text{orifice}}$ as noted by Shi et al. (33). The measured average gas/liquid contact time, τ , was 52 ms in the reactor.

Figure 3 (open circles) displays the ratio K_{DV} determined experimentally as a function of droplet diameter for the given reactor length of 0.32 m. Equations 3 and 4 can be combined to fit experimental values of K_{DV} as a function of d with α as the only fit parameter in eq 3. This is shown in Figure 3 (solid line). It was observed that the value of K_c in the lower range (10–200 μm) was only a weak function of droplet diameter, and the average value of K_c was $(4.7 \pm 0.6) \times 10^{-3}$ m/s. The corresponding value of α was determined to be $(2.2 \pm 0.6) \times 10^{-4}$ for naphthalene at the temperature of our experiments (296 K).

The value of α for naphthalene is less than that for other more soluble organic compounds (33, 34). Estimated value of α for pyrene and anthracene on planar water surfaces by Mmeriki et al. (17) is 1×10^{-5} based on laser-induced-fluorescence measurements, and when converted to K_c gives 5×10^{-4} m/s which is an order of magnitude smaller than that for naphthalene measured in the present work. The measurements by Mmeriki et al. (17) were done in such a manner that the corresponding mass accommodation coefficient α for either pyrene or anthracene could not be extracted from their experiments.

The term

$$\phi(\tau) = 1 - \exp\left\{-K_c \frac{1}{R_H K_{WA}} \frac{6}{d^{\tau}}\right\}$$

in eq 3 is the approach to equilibrium uptake for a droplet in the reactor. For small droplet diameters, $\phi(\tau)$ approaches 1. Hence, $R_H K_{WA}$ determines the value of $K_{DV}(\tau)$ for small diameter droplets. Under these circumstances, $R_H K_{WA}$ increases linearly with decreasing droplet diameter since

$$R_H = 1 + \frac{6}{d} \frac{K_{IA}}{K_{WA}}$$

This is shown in Figure 3 (solid line) where K_{DV} exceeds K_{WA} at diameters less than 50 μm . However, when adsorption to the droplet surface is neglected ($R_H = 1$), Figure 3 (broken line) shows that K_{DV} approaches a constant equilibrium value at small droplet diameters given by K_{WA} . This observation corroborates our starting hypothesis that estimates of droplet uptake will be underestimated without surface adsorption consideration for small-diameter droplets. It should be noted that the fitted values of K_{DV} for $d < 50 \mu\text{m}$ were slightly smaller than experimentally observed values, whereas those for $d > 50 \mu\text{m}$ were slightly larger than experimental values. There is the possibility of heterogeneous nucleation of naphthalene due to evaporation of water. Smolik and Schwarz (39) reported that the evaporation of large stationary water drops (1–2-mm diameter) in a mixture of steam and naphthalene vapor resulted in heterogeneous condensation of naphthalene vapor as a supercooled liquid even at temperatures below the melting point of naphthalene. However, in the present experiments water evaporation was not observed and hence this mechanism was discounted.

The value of α is a function of temperature. Using the nucleation model for uptake into droplets it has been shown that the following relationship describes the temperature dependence of α for the transition state between the gas and the solvated cluster (23)

$$\ln\left(\frac{\alpha}{1-\alpha}\right) = -\frac{\Delta_{\text{obs}} H^0}{R} \frac{1}{T} + \frac{\Delta_{\text{obs}} S^0}{R} \quad (5)$$

Therefore, a plot of $\ln(\alpha/(1-\alpha))$ versus $1/T$ will give the standard enthalpy as the slope and entropy as the intercept (Figure 4). The resulting values are shown in Table 2. It is

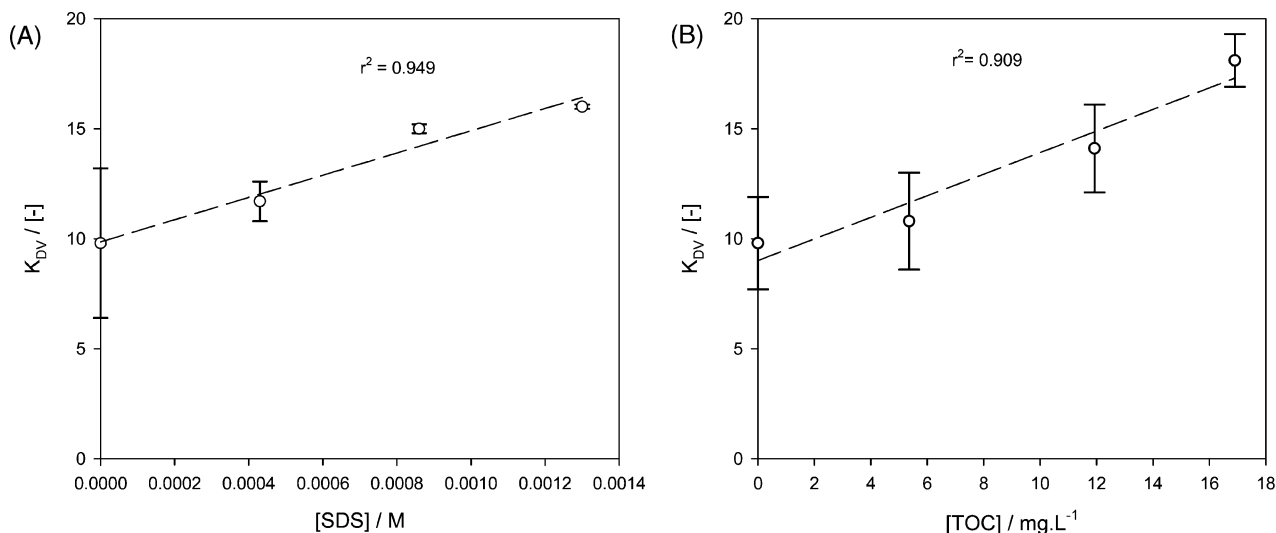


FIGURE 5. Effects of (A) dissolved SDS and (B) dissolved SFA on the droplet–vapor partition constant for naphthalene on a 95- μm water droplet. Lines are merely linear fits to the data.

TABLE 2. Enthalpy and Entropy Associated with Mass Accommodation for Naphthalene

enthalpy of mass accommodation, $\Delta_{\text{obs}}H^{\circ}$	-123 kJ·mol ⁻¹
entropy of mass accommodation, $\Delta_{\text{obs}}S^{\circ}$	-482 J·K ⁻¹ ·mol ⁻¹

interesting to compare the enthalpy of mass accommodation, which is negative (exothermic) with the excess enthalpy of solution reported to be +2.3 kJ·mol⁻¹ (19). The excess enthalpy of solution is a measure of the interaction between the solute and water, and positive values indicate low solubility. This indicates that considerably less energy is required to form the cluster at the surface than it is to completely solvate a hydrophobic PAH molecule in water. The entropy associated with mass accommodation is also largely negative just as the entropy of dissolution, indicating the unfavorable nature of the local structuring of water molecules induced by the solute in both clustering and complete solvation. Similar arguments and observations have also been put forward for the mass accommodation of other aromatic compound types such as phenol and substituted phenols (33).

In addition to the effect of temperature on α , it also affects the value of K_{IA} . As was noted earlier decreased temperature increased the value of K_{IA} for compounds that have an exothermic value of the enthalpy of adsorption. For example, the K_{IA} value for naphthalene at a subambient temperature of 10 °C is 113 μm as compared to 27 μm at 25 °C. Therefore, at the low temperature K_{DV} will increase and therefore a higher concentration in the droplet will result.

The situation in the natural atmosphere is complicated by the fact that fog contains a significant fraction of organic matter (OM), some of which is surface active (39, 40). This increases the dissolved concentration of PAHs that associate with OM and adds to the overall load of PAHs in fog. In an attempt to understand the effects of dissolved surface-active material in the droplet on naphthalene vapor uptake, we conducted a few experiments using a typical anionic surfactant (sodium dodecyl sulfate, SDS) and a dissolved organic carbon (Suwanee Fulvic Acid, SFA) in water. SFA has been shown to be a good reference compound for humic-like materials in clouds, fogwaters, and water-aerosol extracts (42). Figure 5 shows our data on K_{DV} for naphthalene on a 95- μm droplet at 296 K in the falling droplet apparatus. It is clear that K_{DV} increases linearly with increasing SDS and SFA (total organic carbon) concentrations investigated. SDS adsorbs on the surface of the droplet with its hydrocarbon tail exposed to air. Increasing SDS surface coverage makes the droplet surface more hydrophobic thereby promoting adsorption and uptake of naphthalene vapor. Recent works by others (17, 41) have shown that on a planar organic-coated water surface the adsorption of pyrene and anthracene is enhanced 2 to 3 times that on a pure water surface. This provides further proof that organic surface-active films on fog droplets may modify the uptake of hydrophobic organic vapors.

The overall conclusion is that for micron-size fog droplets the increased organic matter and increased air/water interfacial adsorption at subambient temperatures would lead to a significant fog depositional flux of aromatic hydrocarbon vapors from the lower atmosphere (38). Further field measurements of PAHs in size fractionated fog droplets are necessary to confirm these predictions.

Acknowledgments

This work was supported by a grant from the National Science Foundation (ATM-0082836). We thank Dr. S. Ekkad and Mr. R. Hebert of the Mechanical Engineering Department for the use of their fast photography techniques. We also thank

Dr. K. Murray, Department of Chemistry, and Dr. R. Kurtz and Mr. J. Toups, Department of Physics, for the use of the frequency generators. Dr. J. Caprio and Mr. S. Rolan of the Department of Biological Sciences are thanked for allowing us the use of the capillary-pull apparatus.

Literature Cited

- Bernstein, M. P.; Sandford, S. A.; Allamandola, L. J. *Sci. Am.* **1999**, *42*, 281.
- Fernandez, P.; Vilanova, R. M.; Grimalt, J. O. *Environ. Sci. Technol.* **1999**, *33*, 3716–3722.
- Laflamme, R. E.; Hites, R. A. *Geochim. Cosmochim. Acta* **1978**, *42*, 289–303.
- Kawamura, K.; Suzuki, I. *Naturwissenschaften* **1994**, *81*, 502–505.
- Masclat, P.; Hoyau, V.; Jaffrezo, J. L.; Cachler, H. *Atmos. Environ.* **2000**, *34*, 3195–3207.
- Lima, A. L. C.; Eglington, T. I.; Reddy, C. M. *Environ. Sci. Technol.* **2003**, *37*, 53–61.
- Subramanyam, V.; Valsaraj, K. T.; Thibodeaux, L. J.; Reible, D. D. *Atmos. Environ.* **1994**, *28*, 3083–3091.
- Schwarzenbach, R. P.; Gschwend, P. M.; Imboden, D. M. *Environmental Organic Chemistry*, 2nd ed.; John Wiley & Sons: New York, 2002.
- Pankow, J. M. *Atmos. Environ.* **1997**, *31*, 927–929.
- Costanza, M. S.; Brusseau, M. L. *Environ. Sci. Technol.* **2000**, *34*, 1–11.
- Hartkopf, A.; Karger, B. L. *Acc. Chem. Res.* **1973**, *6*, 209–216.
- Braunt, B. H.; Conklin, M. H. *Environ. Sci. Technol.* **2001**, *35*, 362–364.
- Valsaraj, K. T. *Chemosphere* **1988**, *17*, 875–887.
- Hoff, J. T.; Mackay, D.; Gillham, R.; Shiu, W. Y. *Environ. Sci. Technol.* **1993**, *27*, 2174–2180.
- Roth, C. M.; Goss, K.-U.; Schwarzenbach, R. P. *J. Colloid Interface Sci.* **2002**, *252*, 21–30.
- Donaldson, D. J.; Anderson, D. J. *Phys. Chem. A* **1999**, *103*, 871–876.
- Mmerekki, B. T.; Chaudhuri, S. R.; Donaldson, D. J. *J. Phys. Chem. A* **2003**, *107*, 2264–2269.
- Girardet, C.; Toubin, C. *Surf. Sci. Rep.* **2001**, *44*, 159–238.
- Raja, S.; Yaccone, F. S.; Ravikrishna, R.; Valsaraj, K. T. *J. Chem. Eng. Data* **2002**, *47*, 1213–1219.
- Valsaraj, K. T.; Raja, S.; Andrews, T.; Kommalapati, R. R.; Ravikrishna, R. *Proceedings of the AWMA 96th Annual Conference Exhibition, 2003*.
- Smith, J. S.; Valsaraj, K. T. *Chem. Eng. Prog.* **1998**, *94* (5), 69–76.
- Mackay, D.; Shiu, W. Y.; Valsaraj, K. T.; Thibodeaux, L. J. *Air–Water Transfer – The Role of Partitioning in Air–Water Mass Transfer*, Wilhelms, S. C., Gulliver, J. S., Eds.; ASCE: New York, 1991.
- Nathanson, G. M.; Davidovits, P.; Worsnop, D. R.; Kolb, C. E. *J. Phys. Chem.* **1996**, *100*, 13007–13020.
- Glotfelty, D. E.; Majewski, M. S.; Seiber, J. N. *Environ. Sci. Technol.* **1997**, *24*, 353–359.
- Capel, P. D.; Leuenberger, C.; Giger, W. *Atmos. Environ.* **1991**, *25*, 1335–1339.
- Valsaraj, K. T.; Thoma, G. J.; Thibodeaux, L. J.; Reible, D. D. *Atmos. Environ.* **1993**, *27*, 203–210.
- Rafson, R. Adsorption: Fog. In *Odor and VOC Control Handbook*; Rafson, H. F., Ed.; McGraw-Hill Book Co.: New York, 1998; Chapter 8.5.2.
- Seinfeld, J. H.; Pandis, S. N. *Atmospheric Chemistry and Physics*, second edition; John Wiley & Sons: New York, 1998.
- Warneck, P. *Chemistry of the Natural Atmosphere*, second edition; Academic Press: New York, 2000.
- Kolb, C. E.; Worsnop, D. R.; Zahniser, M. S.; Davidovits, P.; Keyser, L. F.; Leu, M.-T.; Molina, M. J.; Hanson, D. R.; Ravishankara, A. R.; Williams, L. R.; Tolbert, M. A. Laboratory Studies of Atmospheric Heterogeneous Chemistry. In *Progress and Problems in Atmospheric Chemistry*; Baker, J. R., Ed.; World Scientific: Singapore, 1995; Chapter 15, pp 771–875.
- Ulmke, H.; Meitschke, M.; Bauckhage, K. *Chem. Eng. Technol.* **2001**, *24*, 69–70.
- Jayne, J. T.; Duan, S. X.; Davidovits, P.; Worsnop, D. R.; Zahniser, M. S.; Kolb, C. E. *J. Phys. Chem.* **1992**, *96*, 5452–5455.
- Muller, R.; Heal, M. R. *J. Phys. Chem. A* **2002**, *106*, 5120–5127.
- Sander, S. P.; Friedl, R. R.; Ravishankara, A. R.; Golden, D. M.; Kolb, C. E.; Kurylo, M. J.; Huie, R. E.; Orkin, V. L.; Molina, M.

- J.; Moortgart, G. K.; Finlayson-Pitts, B. J. *Chemical Kinetics and Photochemical Data for Use in Atmospheric Studies*. Evaluation Number 14, JPL Publication 02-25: Jet Propulsion Laboratory: Pasadena, CA, February 1, 2003.
- (35) Valsaraj, K. T. *Elements of Environmental Engineering—Thermodynamics and Kinetics*, 2nd ed.; CRC/Lewis: Boca Raton, FL, 2000.
- (36) Shi, Q.; Li, Q.; Davidovits, P.; Jayne, J. T.; Worsnop, D. R.; Mozurkevich, M.; Kolb, C. E. *J. Phys. Chem. B* **1999**, *103*, 2417–2430.
- (37) Smolik, J.; Schwarz, J. J. *Colloid Interface Sci.* **1997**, *185*, 382–389.
- (38) Wania, F. *Environ. Sci. Technol.* **2003**, *37*, 1344–1351.
- (39) Herckes, P.; Lee, T.; Trenary, L.; Kang, G.; Chang, H.; Collett, J. L. *Environ. Sci. Technol.* **2002**, *36*, 4777–4782.
- (40) Desecari, S.; Facchini, M. C.; Fuzzi, S.; Tagliavini, E. *J. Geophys. Res.* **2000**, *105 D1*, 1481–1489.
- (41) Mmerek, B. T.; Donaldson, D. J. *Phys. Chem. Chem. Phys.* **2002**, *4*, 4186–4191.
- (42) Capiello, A.; De Simoni, E.; Fiorucci, C.; Mangani, F.; Palma, P.; Trufelli, H.; Decesari, S.; Facchini, M. C.; Fuzzi, S. *Environ. Sci. Technol.* **2003**, *37*, 1229–1240.
- (43) <http://webbook.nist.gov/chemistry/>.

Received for review June 12, 2003. Revised manuscript received October 23, 2003. Accepted October 30, 2003.

ES034591F